

The Effects of the Longitudinal Axis of Loading upon Bending, Shear and Torsion of a Thin-Walled Cantilever Channel Beam

David W. A. Rees, Abdelraouf M. Sami Alsheikh

College of Engineering and Design, Brunel University, Uxbridge, UK
Email: David.Rees@brunel.ac.uk, dralsheikh1948@gmail.com

How to cite this paper: Rees, D.W.A. and Alsheikh, A.M.S. (2024) The Effects of the Longitudinal Axis of Loading upon Bending, Shear and Torsion of a Thin-Walled Cantilever Channel Beam. *World Journal of Mechanics*, 14, 73-96.
<https://doi.org/10.4236/wjm.2024.145005>

Received: November 10, 2023

Accepted: May 28, 2024

Published: May 31, 2024

Copyright © 2024 by author(s) and Scientific Research Publishing Inc.
This work is licensed under the Creative Commons Attribution International License (CC BY 4.0).
<http://creativecommons.org/licenses/by/4.0/>



Open Access

Abstract

Three aluminium channel sections of US standard extruded dimension are mounted as cantilevers with x -axis symmetry. The flexural bending and shear that arise with applied axial torsion are each considered theoretically and numerically in terms of two longitudinal axes of loading not coincident with the shear centre. In particular, the warping displacements, stiffness and stress distributions are calculated for torsion applied to longitudinal axes passing through the section's centroid and its web centre. The stress conversions derived from each action are superimposed to reveal a net sectional stress distribution. Therein, the influence of the axis position upon the net axial and shear stress distributions is established compared to previous results for each beam when loading is referred to a flexural axis through the shear centre. Within the net stress analysis is, it is shown how the constraint to free warping presented by the end fixing modifies the axial stress. The latter can be identified with the action of a 'bimoment' upon each thin-walled section.

Keywords

Thin-Aluminium Channels, Cantilever Beam, Bending Shear, Torsion, Warping, Bimoment, Flexural Axis, Centre of Twist, Centroid, Shear Centre, Torsional Stiffness, Constrained Stress

1. Introduction

A pure torsion applied to the longitudinal axis of a thin closed section is referred to the St Venant torsion theory when the ends of a beam are free to carry equal but opposing torques. Here the shear stress in a thin wall and the angular twist between the ends are found from a torsion theory which simplifies to three-part formula: $T = GJd\theta/dz = 2Aq$, when the section is uniform in a single material.

There is no requirement to specify the axis of torsion in that A refers to an area enclosed by the mean wall closed perimeter and the St Venant torsion constant $J = 4A^2 / \int ds/t$ is a property of the cross-section. In the case of a thin-walled open section a different theory applies in which the St Venant torque is supplemented by the Wagner Kappus torque. The latter arises with the change that occurs to the natural warping displacements for the closed tube when the section has an opening. A further alteration to the warping occurs when as, in this paper, torsion is applied to an open section cantilever beam in which one end is clamped to prevent any axial warping displacement from occurring at that end. Moreover, the influence of the clamped fixing extends over the full length to modify the 'free' warping displacements that would otherwise be found under torsion of an open section beam with unclamped ends. The influence of the axis of torsion upon a clamped-end cantilever beam is investigated here following previous analysis [1] of this beam where the torsion was applied at the free end about the beam's flexural axis. Where the beam section is uniform throughout the length the flexural axis refers to a straight longitudinal axis through the shear centre at every section of the beam. The analyses are complicated by the fixing involving: (1) the location of the position of the beam section's shear centre; (2) calculation of the axial stress distribution in the thin walls due to the beam's fixed-end constraint and (3) accounting for the corresponding increase in torsional stiffness between the ends due to the end fixing. No flexure (bending and transverse shear) occurs with torsion applied to the axis at \mathbf{E} provided that axis coincides with the length axis at the section's centre of twist. The latter axis refers to points in the cross-section that do not rotate. The assumption of coincidence between axes at the centres of twist and shear is often made [2] but has been questioned from a minimal energy condition imposed by an absence of rotation. Other approaches might test the assumption of co-incidence more directly, as here, when the axis of torsion is deliberately shifted away from \mathbf{E} . Here, two further torsion axes are considered: one through the section's centroid \mathbf{G} and the other through the web centre \mathbf{O} . By implication points along torsion axes passing through \mathbf{G} and \mathbf{O} will rotate and thereby influence the behaviour listed above in (1)-(3). The many equations required to reveal the trends that each shift involves are summarised below. These are applied to three standard US channel sections mounted with the web in a vertical disposition carrying two, equal length, horizontal flanges.

Equation Summary

The equations listed below are used for the calculations that follow. The derivations of all equations can be found in [1]. Here certain equations have been adapted often in non-dimensional form to the specific US Imperial dimensions of the three channel sections investigated. For example, $(GJ/Td^2)w$ appears as the chosen non dimensional measure of small warping displacements allowing the physical displacement w to be calculated from material and sectional constants: G , J , and d , under a given torque T . Similarly, the primary warping constant Γ_1 takes a normalised form: $\Gamma_1/(ta^2d^3)$ in which a , d and t are section dimensions.

$$\begin{aligned}
AX' &= \sum A_i X_i \\
\Gamma_1 &= \int y^2 t ds - \bar{y}^2 \int_s t ds \\
J &= \frac{1}{3} \sum b t^3 \\
\mu^2 &= GJ/EG\Gamma_1 \\
T/G\theta &= \left[\mu J (1 + \exp(-2\mu L)) \right] / \left[(\mu L - 1) + (\mu L + 1) \exp(-2\mu L) \right] \\
GJw_o/T &= -(y - \bar{y}) = -2A_E \\
w &= w_o \left[1 - \cosh \mu(L - z) / \cosh \mu L \right] \\
w &= w_o (1 - 1/\cosh \mu L), \text{ for } z = L \\
w_o &= -(T/GJ)(y - \bar{y}) = -2A_E(T/GJ)
\end{aligned}$$

Rate of Twist

$$d\theta/dz = (T/GJ) \left[1 - \cosh \mu(L - z) / \cosh \mu L \right]$$

Integrating *w. r. t. z* for $\theta(z)$:

$$\theta(z) = (T/GJ) \left\{ z + \left[\sinh \mu(L - z) - \sinh \mu L \right] / \mu \cosh \mu L \right\}$$

For $z = L$, this will result

$$\begin{aligned}
\theta(L) &= (T/GJ) \left[1 - (\mu L)^{-1} \tanh \mu L \right] \\
\theta(L) &= (TL/GJ) \left[(\mu L - 1) + (\mu L + 1) e^{-2\mu L} \right] / \mu L (1 + e^{-2\mu L}) \\
&= (T/GJ\mu) \left[(\mu L - 1) + (\mu L + 1) e^{-2\mu L} \right] / (1 + e^{-2\mu L})
\end{aligned}$$

Stress Constraint

$$\sigma_z = E dw/dz = -E \times d(2A_E d\theta/dz)/dz$$

in which, from Equation (8a)

$$\begin{aligned}
d^2\theta/dz^2 &= (T/GJ) \left[\mu \sinh \mu(L - z) / \cosh \mu L \right] \\
\sigma_z &= -2A_E E (d^2\theta/dz^2) = -2A_E E \theta'' \\
&= (-2A_E ET/GJ) \left[\mu \sinh \mu(L - z) / \cosh \mu L \right]
\end{aligned}$$

Alternatively, with $\mu^2 = GJ/EG\Gamma_1$:

$$\begin{aligned}
\sigma_z &= (-2A_E ET/\mu\Gamma_1) \left[\sinh \mu(L - z) / \cosh \mu L \right] \\
\sigma_z &= (-2A_E ET/GJ) \left[\mu \sinh \mu(L - z) / \cosh \mu L \right]
\end{aligned}$$

and from Equation (7b):

$$\sigma_z = Ew_o \left[\mu \sinh \mu(L - z) / \cosh \mu L \right]$$

Equation (8a) applies to $0 \leq z \leq L$

$$\sigma_z = -(2A_E T/\mu\Gamma_1) \left[\sinh \mu(L - z) / \cosh \mu L \right]$$

which attains its maximum for $z = 0$

$$\sigma_z = (-2A_E T/\mu\Gamma_1) \tanh \mu L$$

$$\sigma_z = (-2A_E T / \mu \Gamma_1) \times (1 - e^{-2\mu L}) / (1 + e^{-2\mu L})$$

$$\sigma_z = -(y - \bar{y}) T / \mu \Gamma_1 \times (1 - e^{-2\mu L}) / (1 + e^{-2\mu L})$$

$$\sigma_z = (\bar{y} - y) T / \mu \Gamma_1 \times (1 - e^{-2\mu L}) / (1 + e^{-2\mu L})$$

2. Channel Section—Axial Torsion at Centroid G

This section and the next examine the effect of a shift in the axis of torsion, away from the shear centre, upon the unconstrained warping displacements. Firstly, the axis is shifted from the shear centre E to pass through the channel’s centroid **G**. The position X' of **G** from the web centre in the X direction (see **Figure 1**) follows from Equation (1) given above as:

$$AX' = \sum A_i X_i \tag{1}$$

$$(dt + 2at) X' = 2(at \times a/2)$$

$$X' = a^2 / (d + 2a)$$

Here (twice) the swept areas A_G are required between **G** and the section’s perimeter points 1, 2, 3, ..., 7 in **Figure 1(a)**.

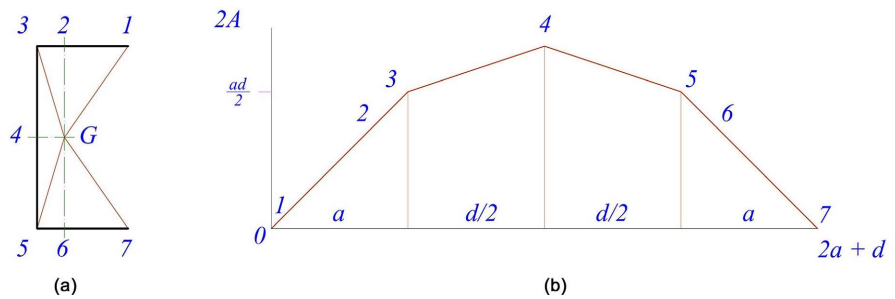


Figure 1. Channel section with swept areas taken from centroid G.

Three calculations are sufficient to construct the swept area plot given in **Figure 1(b)**. Starting from the free edge at position 1, the three triangular areas are identified:

$$A_{G13} = 2[(a/2) \times (d/2)] = ad/2$$

$$A_{G34} = 2 \times (X'/2) \times (d/2) = a^2 d / 2(a + d)$$

$$A_{134} = A_{G13} + A_{G34} = 2 = (ad/2)(d + 3a) / (d + 2a)$$

from which the mean co-ordinate \bar{y} for **Figure 1(b)** follows:

$$\int_s \bar{y} ds = \int_s y ds$$

$$(2a + d) \bar{y} = 2(ad/2 \times a/2) + 2[ad/2 + (ad/2)(d + 3a)/(d + 2a)](d/4)$$

$$\bar{y} = (ad/4)(7ad + 4a^2 + 2d^2) / (2a + d)^2$$

$$\bar{y}/d^2 = (1/4)(a/d)[7(a/d) + 4(a/d)^2 + 2] / [1 + 2(a/d)]^2$$

The straight-line equations: $y = y(s)$, describing the sides of the plot in **Figure 1(b)** and the integrals $\int_s y^2 ds$ for the warping constant, in Equation (2) are evaluated, with t constant, as follows:

1-3 for $0 \leq s \leq a$

$$y = ds/2; \int_s y^2 ds = (d/2)^2 \int_s s^2 ds = (d/2)^2 \times a^3/3 = a^3 d^3/12$$

3-4 for $a \leq s \leq a + d/2$

$$y = ad/2 + a^2 d/2(a+d) \times (2/d)(s-a) = ad/2 + a^2(s-a)/(d+2a)$$

$$\int_s y^2 ds = \int_s \left[ad/2 + a^2(s-a)/(d+2a) \right]^2 ds$$

$$= (ad/2)^2 (d/2) + \left[a^3 d/2(d+2a) \right] (d/2)^2 + (1/3) \left[a^2/(d+2a) \right]^2 (d/2)^3$$

Hence, for the whole cross-section, the two terms appearing in the primary warping constant Γ_1 follow from the summary Equation (2) given above

$$\Gamma_1 = \int_s y^2 t ds - \bar{y}^2 \int_s t ds \quad (2a)$$

where:

$$\int_s y^2 t ds = 2t \left\{ a^3 d^3/12 + (ad/2)^2 (d/2) + \left[a^3 d/2(d+2a) \right] (d/2)^2 + (1/3) \left[a^2/(d+2a) \right]^2 (d/2)^3 \right\}$$

$$= (ta^2 d^3/2) \left[(1/3)(a/d) + 1/2 + (1/2)(a/d)/(1+2a/d) + (1/6)(a/d)^2/(1+2a/d)^2 \right] \quad (2b)$$

$$\bar{y}^2 \int_s t ds = \bar{y}^2 (2a+d)t = \left\{ (ad/4)(7ad+4a^2+2d^2)/(2a+d)^2 \right\}^2 \times (2a+d)t \quad (2c)$$

Equations 2(a)-(c) are applied to the three channel geometries as follows:

Section A: $a = 1/2"$, $d = 1"$, $t = 1/16"$, $L = 300$ mm (11.81")

$a/d = 1/2$, $t/d = 1/16$, $d = 25.4$ mm, $L = 300$ mm. $E = 210$ GPa, $G = 70$ GPa

$$\int_s y^2 t ds = (ta^2 d^3/2) \left[(1/3)(1/2) + 1/2 + (1/2)(1/2)/(1+1) + (1/6)(1/2)^2/(1+1)^2 \right]$$

$$= (77/192) ta^2 d^4$$

$$\bar{y}^2/d^2 = (1/4)(1/2)(7/2 + 4/4 + 1/2)/(1+1)^2 = 13/64$$

$$\bar{y}^2 (2a+d)t = (13d^2/64)^2 (2a+d)t = 169ta^2 d^3/512$$

1) Constants

The following constants are calculated for this Section A.

$$\Gamma_1 = (77/192 - 169/512) ta^2 d^3 = (109/1536) ta^2 d^3 = 0.5677 ta^5 \quad (2)$$

$$\Gamma_1 = (109/1536) \times 1.5875 \times 12.7^2 \times 25.4^3 = 2.9775 \times 10^5 \text{ mm}^6$$

$$J = (2a+d) \left(t^3/3 \right) = 4at^3/3 = (2 \times 12.7 + 25.4) (1.5875^3/3) = 67.746 \text{ mm}^4 \quad (3)$$

$$\mu = \sqrt{GJ/E\Gamma_1} = \sqrt{4at^3/(9 \times 0.5677 ta^5)} = 0.8848 t/a^2 \quad (4)$$

$$\begin{aligned} \mu &= \sqrt{(70 \times 10^3 \times 67.746) / (210 \times 10^3 \times 2.9775 \times 10^5)} = 8.71 \times 10^{-3} \text{ mm}^{-1} \\ \mu L &= 0.8848(t/a)(L/a) = 0.8848(1/8)(300/12.7) = 2.613 \\ \exp(-2\mu L) &= \exp(-5.226) = 5.375 \times 10^{-3} \\ \cosh \mu L &= \cosh 2.613 = 6.857 \\ \cosh(\mu L/2) &= \cosh 1.307 = 1.983 \end{aligned}$$

2) Torsional Stiffness

$$\begin{aligned} T/G\theta &= [\mu J(1 + \exp(-2\mu L))] / [(\mu L - 1) + (\mu L + 1)\exp(-2\mu L)] \\ &= (0.8848t/a^2) \times (4at^3/3) \times 0.6159 = 0.7266t^4/a \\ \therefore T/\theta &= 0.7266 \times 70 \times 10^3 \times 1.58754/12.7 \\ &= 25.436 \times 10^3 \text{ N} \cdot \text{mm/rad} = 25.436 \text{ N} \cdot \text{m/rad} \end{aligned} \tag{5}$$

3) Unconstrained Warping Displacements

These displacements w_o which are independent of length, follow from

$$GJw_o/T = -(y - \bar{y}) \tag{6}$$

Equation (6) gives at each median point. 1, 3 and 4:

$$(GJ/T)w_{o1} = (GJ/T)w_{o7} = \bar{y}$$

$$(GJ/T)w_{o3} = (GJ/T)w_{o5} = \bar{y} - ad/2$$

$$(GJ/T)w_{o4} = \bar{y} - (ad/2)(d + 3a)/(d + 2a)$$

At 1, $y_1 = 0: (GJ/T)w_{o1} = -(0 - 13d^2/64)$

$$\therefore (GJ/Td^2)w_{o1} = 13/64$$

At 3, $y_3 = ad/2: (GJ/Td^2)w_{o3} = -(ad/2 - 13d^2/64)$

$$(GJ/Td^2)w_{o1} = -(a/2d - 13/64) = -(1/4 - 13/64)$$

$$\therefore (GJ/Td^2)w_{o1} = -3/64$$

At 4, $y_3 = (ad/2)(d + 3a)/(d + 2a)$

$$(GJ/T)w_{o4} = -[(ad/2)(d + 3a)/(d + 2a) - 13d^2/64]$$

$$(GJ/Td^2)w_{o4} = -[(1/2)(a/d)(1 + 3a/d)/(1 + 2a/d) - 13/64]$$

$$= -[(1/2)(1/2)(1 + 3/2)/(1 + 1) - 13/64]$$

$$= -(5/16 - 13/64)$$

$$\therefore (GJ/Td^2)w_{o4} = -7/64$$

4) Constrained Warping Displacements

With one end fully constrained these displacements $w = w(z)$ follow from Equations (7a), (7b):

$$w = w_o [1 - \cosh \mu(L - z) / \cosh \mu L] \tag{7a}$$

for which, with $z = L$ at the free-end, the constrained warping displacements become:

$$w = w_o (1 - 1/\cosh \mu L) \tag{7b}$$

in which the multiplication factor $(1 - 1/\cosh \mu L)$ in Equation (7b) modifies the unconstrained warping displacement w_o at the free end

$$w = w_o (1 - 1/6.857) = 0.854w_o$$

The warping constraint increases towards the fixing. At the fixed-end the cross-section becomes fully constrained in that there are no warping displacements. At the mid-length position Equation (7a) shows for $z = L/2$

$$w = w_o [1 - \cosh(\mu L/2)/\cosh \mu L]$$

$$w = w_o (1 - 1.983/6.857) = 0.711w_o$$

Table 1 applies the coefficients 0.854 and 0.711 to w_o giving the *constrained* warping displacements at the end and centre lengths at points 1, 2 and 3 in this section.

Table 1. Warping displacements at the free-end and centre lengths with torque at **G** for Section **A**.

↓ Position/Point →	1	3	4
Unconstrained Free End: $(GJ/Td^2)w_o =$	13/64	-3/64	-7/64
at $z = L$, $0.854(GJ/Td^2)w_o = (GJ/Td^2)w =$	0.1735	-0.040	-0.0934
at $z = L/2$, $0.711(GJ/Td^2)w_o = (GJ/Td^2)w =$	0.1444	-0.0333	-0.0778

To read from **Table 1** if, say, the constrained displacement is required for point 1 at mid length under an axial torque of 1 Nm then the coefficient of 0.1444 appears within the conversion of the normalised displacement as follows

$$\begin{aligned} w_1 &= 0.711 \times (13/64) \times Td^2/GJ \\ &= 0.1444 \times (1 \times 10^3) \times 25.4^2 / [(70 \times 10^3) \times 67.746] \\ &= 1.965 \times 10^{-3} \text{ mm} \end{aligned}$$

The constrained warping distribution for this section is examined further in the summary that follows in § 3.

Section B: $a/d = 4/7$, $t/d = 1/14$, $d = 44.45 \text{ mm}$, $L = 1 \text{ m}$

$$a = 1", d = 1\frac{3}{4}", t = 1/8", L = 1 \text{ m} (39.37")$$

$$\bar{y}/d^2 = (1/4)(4/7) [7(4/7) + 4(4/7)^2 + 2] / (1 + 8/7)^2 = 358/1575$$

$$\bar{y}^2 (2a + d)t = (358d^2/1575)^2 (2a + d)t = (105/16)(358/1575)^2 ta^2d^3$$

$$\begin{aligned} \int_s y^2 t ds &= (ta^2d^3/2) [(1/3)(4/7) + 1/2 + (1/2)(4/7)/(1 + 8/7) \\ &\quad + (1/6)(4/7)^2 / (1 + 8/7)^2] \\ &= (7897/9450)(ta^2d^3/2) \end{aligned}$$

$$\Gamma_1 = [(7897/9450) - (105/8)(358/1575)^2] (ta^2d^3/2) = 0.07877ta^2d^3$$

1) Constants

$$\Gamma_1 = 0.07877 \times 3.175 \times 25.4^2 \times 44.45^3 = 14.17 \times 10^6 \text{ mm}^6$$

$$J = (2a + d)(t^3/3) = (2 \times 25.4 + 44.45)(3.175^3/3) = 1016.19 \text{ mm}^4$$

$$\begin{aligned} \mu &= \sqrt{GJ/E\Gamma_1} \\ &= \sqrt{(70 \times 10^3 \times 1016.19)/(210 \times 10^3 \times 14.17 \times 10^6)} \\ &= 4.889 \times 10^{-3} \text{ mm}^{-1} \end{aligned}$$

$$\mu L = 4.889 \times 10^{-3} \times 1000 = 4.889$$

$$\exp(-2\mu L) = \exp(-9.778) = 56.68 \times 10^{-6}$$

$$\cosh \mu L = \cosh 4.889 = 66.414$$

$$\cosh(\mu L/2) = \cosh 2.445 = 5.809$$

2) Torsional Stiffness

$$\begin{aligned} T/\theta &= [\mu GJ(1 + \exp(-2\mu L))] / [(\mu L - 1) + (\mu L + 1)\exp(-2\mu L)] \\ &= [(4.889 \times 10^{-3}) \times (70 \times 10^3) \times 1016.89(1 + \exp(-9.778))] / [3.889 + 5.889 \exp(-9.778)] \\ &= 89.42 \times 10^3 \text{ N} \cdot \text{mm/rad} = 89.42 \text{ N} \cdot \text{m/rad} \end{aligned}$$

3) Unconstrained Warping Displacements w_o

From Equation (6):

$$GJw_o/T = -(y - \bar{y})$$

giving at each 'corner' position:

$$(GJ/T)w_{o1} = (GJ/T)w_{o5} = \bar{y}$$

$$(GJ/T)w_{o2} = (GJ/T)w_{o4} = \bar{y} - ad/2$$

$$(GJ/T)w_{o3} = \bar{y} - d(a + e)/2$$

$$\text{At 1, } y_1 = 0: (GJ/T)w_{o1} = -(0 - 358d^2/1575)$$

$$\therefore (GJ/T)w_{o1} = 0.2273$$

$$\text{At 3, } y_3 = ad/2: (GJ/T)w_{o3} = -(ad/2 - 358d^2/1575)$$

$$(GJ/Td^2)w_{o3} = -(ad/2 - 358/1575) = -(2/7 - 358/1575)$$

$$\therefore (GJ/Td^2)w_{o3} = -0.0584$$

$$\text{At 4, } y_4 = (ad/2)(d + 3a)/(d + 2a)$$

$$(GJ/T)w_{o4} = -[(ad/2)(d + 3a)/(d + 2a) - 358d^2/1575]$$

$$(GJ/Td^2)w_{o4} = -[(1/2)(a/d)(1 + 3a/d)/(1 + 2a/d) - 358/1575]$$

$$(GJ/Td^2)w_{o4} = -[(1/2)(4/7)(1 + 12/7)/(1 + 8/7) - 358/1575]$$

$$= -(0.3619 - 0.2273)$$

$$(GJ/Td^2)w_{o4} = -0.1346$$

4) Constrained Warping Displacements

Again, these follow from Equation (7a) as:

$$w = w_o \left[1 - \cosh \mu(L - z) / \cosh \mu L \right] \quad (7a)$$

for which, with $z = L$ at the free-end, the constrained warping displacements become (Equation (7b)):

$$w = w_o (1 - 1/\cosh \mu L) \quad (7b)$$

in which the factor $(1 - 1/\cosh \mu L)$ modifies the unconstrained warping displacements at the free end according to:

$$w = w_o (1 - 1/66.414) = 0.9849w_o$$

showing the 1 m length almost preserves w_o at the free-end. However, the constraint increases towards the fixing. At the fixed end the cross-section becomes fully constrained in that there are no warping displacements. At the mid-length position Equation (7a) shows, for $z = L/2$:

$$w = w_o \left[1 - \cosh(\mu L/2) / \cosh \mu L \right] = w_o (1 - 5.809/66.414) = 0.9125w_o$$

The coefficients 0.9849 and 0.9125 for the end and centre lengths are applied to the free warping displacements w_o at median points 1, 3 and 4 in the section. **Table 2** gives the *constrained* warping displacements within the cross-section at the end and centre lengths at each position.

Table 2. Free-end and centre warping displacements for channel Section **B** with torque at **G**.

↓ Position/Point →	1	3	4
Unconstrained Free End: $(GJ/Td^2)w_o =$	0.2273	-0.0584	-0.1346
at $z = L$, $0.9849(GJ/Td^2)w_o = (GJ/Td^2)w =$	0.2239	-0.0575	-0.1326
at $z = L/2$, $0.9125(GJ/Td^2)w_o = (GJ/Td^2)w =$	0.2074	-0.0533	-0.1228

To read from **Table 2**, say the constrained displacement at point 3 is required at mid-length for a torque of 1 Nm then the coefficient of -0.0533 appears in calculating w_3 as follows:

$$w_o = -0.0584 \times Td^2 / GJ$$

$$w_3 = 0.9125w_o$$

$$w_3 = -0.9125 \times 0.0584 \times Td^2 / GJ$$

$$w_3 = -0.0533 \times (1 \times 10^3) \times 44.45^2 / (70 \times 10^3) \times 1016.19 = -1.48 \times 10^{-3} \text{ mm}$$

Section C: $a/d = 1/3$, $t/d = 1/40$, $d = 47.625 \text{ mm}$, $L = 340 \text{ mm}$

$$a = 5/8", d = 1\frac{7}{8}", t = 3/64", L = 340 \text{ mm} (13.39")$$

$$\bar{y}/d^2 = (1/4)(1/3) \left[7(1/3) + 4(1/3)^2 + 2 \right] / (1 + 2/3)^2 = 43/300$$

$$\begin{aligned}\bar{y}^2 (2a+d)t &= (43d^2/300)^2 (2a+d)t = (45/3)(43/300)^2 ta^2d^3 \\ \int_s y^2 t ds &= (ta^2d^3/2) \left[(1/3)(1/3) + 1/2 + (1/3)/(10/3) + (1/9 \times 9)/(6 \times 25) \right] \\ &= (323/450)(ta^2d^3/2)\end{aligned}$$

1) Constants

$$\begin{aligned}\Gamma_1 &= \left[323/450 - 30(43/300)^2 \right] ta^2d^3/2 = 0.05072ta^2d^3 \\ \Gamma_1 &= 0.05072 \times 1.1906 \times 15.875^2 \times 47.625^3 = 1.644 \times 10^6 \text{ mm}^6 \\ J &= (2a+d)(t^3/3) = (2 \times 15.875 + 47.625)(1.1906^3/3) = 44.654 \text{ mm}^4 \\ \mu &= \sqrt{GJ/E\Gamma_1} = \sqrt{(70 \times 10^3 \times 44.654) / (210 \times 10^3 \times 1.644 \times 10^6)} \\ &= 3.009 \times 10^{-3} \text{ mm}^{-1} \\ \mu L &= 3.009 \times 10^{-3} \times 340 = 1.023 \\ \exp(-2\mu L) &= \exp(-2.046) = 0.1292 \\ \cosh \mu L &= \cosh 1.023 = 1.5705 \\ \cosh(\mu L/2) &= \cosh 0.5115 = 1.1337\end{aligned}$$

2) Torsional Stiffness

$$\begin{aligned}T/\theta &= \left[\mu GJ(1 + \exp(-2\mu L)) \right] / \left[(\mu L - 1) + (\mu L + 1)\exp(-2\mu L) \right] \\ &= \left[(3.009 \times 10^{-3}) \times (70 \times 10^3) \times 44.654(1 + 0.1292) \right] / \left[(1.023 - 1) + (1.023 + 1)0.1292 \right] \\ T/\theta &= 37.35 \times 10^3 \text{ N} \cdot \text{mm/rad} = 37.35 \text{ N} \cdot \text{m/rad}\end{aligned}$$

3) Unconstrained Warping Displacements

From Equation (6):

$$GJw_o/T = -(y - \bar{y})$$

giving at each median= point 1, 3 and 4:

$$(GJ/T)w_{o1} = (GJ/T)w_{o7} = \bar{y}$$

$$(GJ/T)w_{o3} = (GJ/T)w_{o5} = \bar{y} - ad/2$$

$$(GJ/T)w_{o4} = \bar{y} - d(a+e)/2$$

$$\text{At 1, } y_1 = 0: (GJ/T)w_{o1} = -(0 - 43d^2)/300$$

$$\therefore (GJ/Td^2)w_{o1} = 43/300$$

$$\text{At 3, } y_3 = ad/2: (GJ/T)w_{o3} = -(ad/2 - 43d^2/300)$$

$$(GJ/Td^2)w_{o1} = -(a/2d - 43/300) = -\left[(1/2)(1/3) - 43/300 \right]$$

$$\therefore (GJ/Td^2)w_{o1} = -7/300$$

$$\text{At 4, } y_4 = (ad/2)(d+3a)/(d+2a)$$

$$(GJ/T)w_{o4} = -\left[(ad/2)(d+3a)/(d+2a) - 43d^2/300 \right]$$

$$\begin{aligned}
 (GJ/Td^2)w_{o4} &= -[(1/2)(a/d)(1+3a/d)/(1+2a/d)-43/300] \\
 &= -[(1/2)(1/3)(1+1)/(1+2/3)-43/300] \\
 &= -(1/5-43/300) \\
 \therefore (GJ/Td^2)w_{o4} &= -17/300
 \end{aligned}$$

4) Constrained Warping Displacements

Equation (7a) provides w from knowing w_o in 3 above

$$w = w_o [1 - \cosh \mu(L - z) / \cosh \mu L]$$

for which, with $z = L$ at the free-end, the constrained warping displacement Equation (7b) becomes:

$$w = w_o (1 - 1/\cosh \mu L)$$

in which the factor $(1 - 1/\cosh \mu L)$ modifies the unconstrained warping displacements at the free end to

$$w = w_o (1 - 1/1.5705) = 0.3633w_o$$

showing that fixing one end of the 340 mm length constrains the free-end warping to $0.3633w_o$. The constraint increases further towards the fixing where there is no warping when the cross-section becomes fully constrained. At the mid-length position Equation (7a) shows for $z = L/2$

$$\begin{aligned}
 w &= w_o [1 - \cosh \mu(L - z) / \cosh \mu L] \\
 w &= w_o (1 - 1.1337/1.5705) = 0.2781w_o
 \end{aligned}$$

The coefficients 0.3633 and 0.2781 for the end and centre lengths are applied to the free warping displacements w_o at points 1, 3 and 4 in section C. **Table 3** gives the *constrained* warping displacements within the cross-section at the end and centre lengths at each position.

Table 3. Free-end and centre warping displacements for channel Section C with torque at G.

↓ Position/Point →	1	3	4
Unconstrained Free End: $(GJ/Td^2)w_o =$	43/300	-7/300	-17/300
at $z = L$, $0.3633(GJ/Td^2)w_o = (GJ/Td^2)w =$	0.0521	-0.0085	-0.0206
at $z = L/2$, $0.2781(GJ/Td^2)w_o = (GJ/Td^2)w =$	0.0399	-0.0065	-0.01576

To read from **Table 3**, say if the constrained displacement at point 4 is required at mid-span for a torque of 1 Nm then the coefficient of -0.01576 appears in calculating w_4 as follows

$$\begin{aligned}
 w_4 &= 0.2781w_o = 0.2781 \times (-17/300) \times Td^2 / GJ \\
 &= -0.01576 \times (1 \times 10^3) \times 47.625^2 / (70 \times 10^3 \times 44.654) \\
 &= -11.436 \times 10^{-3} \text{ mm}
 \end{aligned}$$

2.1. Torsional Axis Shift from E to G

Figure 2 shows the typical distribution of unconstrained (free) warping displacements for each of the three channel Sections A, B and C per unit torque (1 Nm) applied about the longitudinal centroidal axis through G. The ordinates to the diagram as applied to each section are given in Table 4. It will be seen these displacements are different from those with the torque applied at the shear centre E (see here Figures 3(a)-(c)).

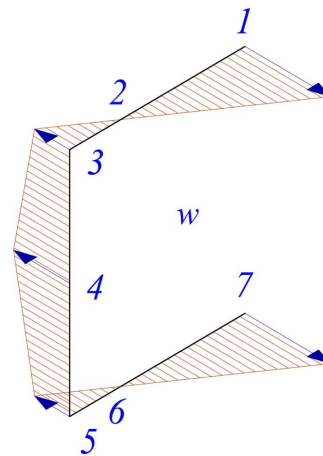


Figure 2. Unconstrained warping for channel cantilever with torque applied about longitudinal centroidal axis.

Table 4. ‘Unconstrained’ warping displacements for channel Sections A, B and C with torque at G.

↓ Section/Point →	1	3
A: $(GJ/Td^2)w_o =$	13/64	-3/64
B: $(GJ/Td^2)w_o =$	0.2273	-0.0584
C: $(GJ/Td^2)w_o =$	43/300	-7/300

To read from Table 4, say if the unconstrained displacements at points 1, 3 and 4 are required for a torque of 1 Nm applied to Section C, then the corresponding coefficients in Table 4 appear in the respective calculations:

$$w_1 = 43 / 300 \times Td^2 / GJ = 43 / 300 \times (1 \times 10^3) \times 47.625^2 / (70 \times 10^3 \times 44.654) = 104 \times 10^{-3} \text{ mm}$$

$$w_3 = -7 / 300 \times Td^2 / GJ = -7 / 300 \times (1 \times 10^3) \times 47.625^2 / (70 \times 10^3 \times 44.654) = -16.93 \times 10^{-3} \text{ mm}$$

$$w_4 = -17 / 300 \times Td^2 / GJ = -17 / 300 \times (1 \times 10^3) \times 47.625^2 / (70 \times 10^3 \times 44.654) = -41.1 \times 10^{-3} \text{ mm}$$

It is seen that the free warping at point 4 has been reduced from -0.0411 mm to -0.0114 mm by constraining one end (see example from Table 3 above).

The difference in unconstrained warping w_o arising from a shift in T from **E** to **G** cannot be explained from static force equilibrium. That is, the torque, when constituted as a couple, may be centred at any position along the horizontal axis including both **E** and **G** and the web centre (to follow). It is the change to the in-plane displacements u and v that the shift involves which explains the difference in w_o . With the exception of the centre point of twist, every other point in the section is displaced by u and v in the directions of x and y respectively [2] [3] [4]. Taking the shear centre to coincide with the centre of twist [5] [6] then **E** does not rotate under T but all other points including **G** do. Therefore, a rotation applies when T is applied at **G**. With T applied at **E**, also identified as the section's principal pole position, the swept areas refer to pure torsion [7] [8]. When T is applied at **G** the swept areas refer to torsion combined with bending displacements u and v . Thus, it is the contribution from bending that alters warping with the shift in T from **E** to **G**. The corresponding differences between the free warping displacement distributions for each of the three channel sections may be calculated from subtracting the ordinates (see **Figure 2** and **Table 4**) with T applied at **G** from those with T applied at **E** [1]. These differences are shown for three positions 1, 3 and 4 in each section **A**, **B** and **C** in **Table 5** below.

Table 5. Differences between 'unconstrained' warping displacements $(GJ/Td^2)w_o$ for channel sections **A**, **B** and **C** with torque applied at **E** and **G**.

↓ Section/Point →	1	3	4
A:	$27/128 - 13/64 =$ $1/128$	$-5/128 + 3/64 =$ $1/128$	$-17/128 + 7/64 =$ $-3/128$
B:	$0.235 - 0.2273 =$ 0.008	$-0.0504 + 0.0584 =$ 0.008	$-0.161 + 0.135 =$ -0.026
C:	$27/180 - 43/300 =$ 0.0067	$-3/180 + 7/300 =$ 0.0067	$-13/180 + 17/300 =$ -0.0156

Figure 3(a) applies to unconstrained warping with the torque applied at **E**. **Figure 3(b)** applies to unconstrained warping with the torque applied at **G**. **Table 5** shows that similar difference distributions appear for all sections, as in **Fig. 3c**, when distribution **G** is subtracted from distribution **E**. The symmetry in (a) and (b) reveals, from their difference in (c), a uniform equal displacement along both flanges (points 1, 2 and 3 and 4, 5 and 6). These connect linearly to linear distributions in the web giving a negative maximum displacement at the neutral axis point 4. Positive ordinates in (c) indicate where unconstrained displacements under a torsion applied at **E** exceed those from torsion at **G**.

2.2. Fixed-End Stress Distribution

The shift in the axis of torsion from **E** to **G** will also influence the fixed-end axial stress distribution. For torque T , concentric with the centroidal axis **G**, the stress

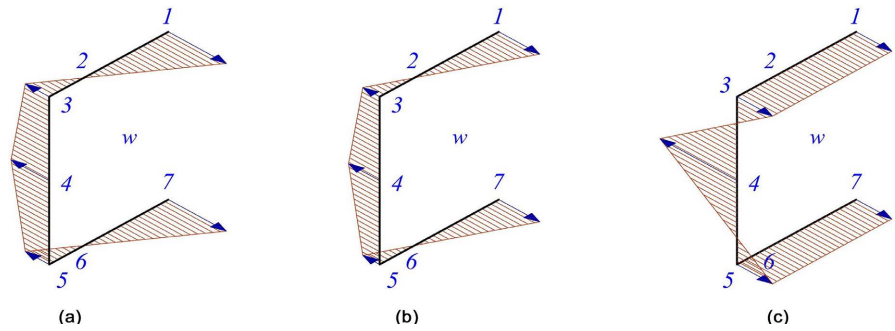


Figure 3. Differences (c) between unconstrained displacements from applying torsion about (a) axes **E** and (b) axis **G**.

constraint in channel section a is found from substitutions appropriate to \bar{y} and Γ_1 [9] [10]. That is:

$$\sigma_z(0) = [(\bar{y} - y)T/\mu\Gamma_1] \times (1 - \exp(-2\mu L)) / (1 + \exp(-2\mu L)) \tag{8}$$

$$\sigma_z(0) = [(\bar{y} - y)T / (0.8887t/a^2) \times (0.5677a^5t)] \times (1 - \exp(-5.428)) / (1 + \exp(-5.428))$$

which is written as:

$$(a^3t^2/T)\sigma_z = 1.9615(13d^2/64 - y)$$

where y is taken from the swept area diagram (see **Figure 1**) for perimeter points 1, 3 and 4:

$$y_1 = 0, (a^3t^2/T)\sigma_{z1} = 1.9615(13a^2/16)$$

$$\therefore (at^2/T)\sigma_{z1} = 1.5937$$

$$y_3 = ad/2, (a^3t^2/T)\sigma_{z3} = 1.9615(13a^2/16 - ad/2)$$

$$\therefore (at^2/T)\sigma_{z3} = -0.3678$$

$$y_4 = (ad/2)(d + 3a)/(d + 2a), (a^3t^2/T)\sigma_{z4} = 1.9615(13a^2/16 - 5a^2/4)$$

$$(at^2/T)\sigma_{z4} = -0.8582$$

A comparison is made in §2.3 between the end-constrained stress distributions with the axes of torsion at **E**, **G** and **O**.

3. Channel Section—Axial Torsion at Web Centre **O**

Here the axial torque is applied to an arbitrary point **O** along an x -axis of symmetry. This point is taken to pass through the web centre (point 4 in **Figure 4(a)**). Warping displacements at points 1, 2, 3, ..., 7 are to be compared with those found previously with the torque axis through the shear centre **E** [1] and through the centroid **G**, given in §1 above.

3.1. Primary Warping Constant

One calculation is sufficient to construct the swept area plot given in **Figure 4(b)**:

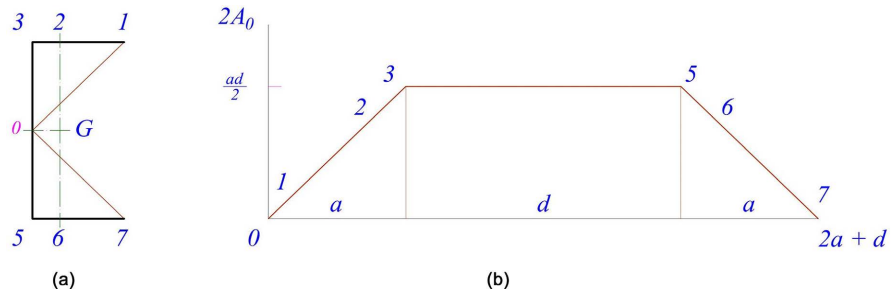


Figure 4. Channel with swept areas taken from web centre O.

$$y = 2A_o = 2(a/2 \times d/2) = ad/2$$

from which the mean co-ordinate \bar{y} follows:

$$\int_s \bar{y} ds = \int_s y ds$$

$$(2a + d)\bar{y} = 2(ad/2 \times a/2) + (ad/2 \times d) = (a + d)ad/2$$

$$\bar{y} = (ad/2)(a + d)/(2a + d)$$

$$\bar{y}/d^2 = (1/2)(a/d)[(a/d) + 1]/[1 + 2(a/d)]$$

The straight-line equations: $y = \gamma(s)$, describing the sides of the plot in Figure 4(b) and the integrals $\int_s y^2 ds$, are as follows:

1-3 for $0 \leq s \leq a$

$$y = ds/2; \int_s y^2 ds = (d/2)^2 \int_s s^2 ds = (d/2)^2 \times a^3/3 = a^3 d^3/12$$

3-4 for $a \leq s \leq a + d/2$

$$y = ad/2; \int_s y^2 ds = (ad/2)^2 \int_s ds = a^2 d^3/8$$

4-5 for $a + d/2 \leq s \leq a + d$

$$y = ad/2; \int_s y^2 ds = (ad/2)^2 \int_s ds = a^2 d^3/8$$

5-7 for $a + d \leq s \leq 2a + d$

$$y = ad/2 - (d/2)[s - (a + d)]; \int_s y^2 ds = (d/2)^2 \int_s [(a + d) - s]^2 ds = a^3 d^2/12$$

Hence, for the whole cross-section the two terms defining the primary warping constant follow from Equation (2):

$$\begin{aligned} \Gamma_1 &= \int_s y^2 t ds - \bar{y}^2 \int_s t ds \\ &= 2t(a^3 d^2/12 + a^2 d^3/8) - [(ad/2)(a + d)/(2a + d)]^2 \times t(2a + d) \end{aligned}$$

$$\Gamma_1/t a^2 d^3 = 2[(1/12)(a/d) + 1/8] - (d/a)(2 + d/a) \times (1/4)(a/d)^2 (1 + 2a/d)^2$$

3.2. Unconstrained Warping

The warping displacement w is found in Equation (6)

$$GJw_o/T = -(y - \bar{y})$$

giving at each of the 'corner' position 1 and 3:

$$(GJ/T)w_1 = (GJ/T)w_7 = \tilde{y}$$

$$(GJ/T)w_3 = (GJ/T)w_4 = (GJ/T)w_5 = \tilde{y} - ad/2$$

The following constants and equations are applied to each channel that follows:

Section A: $a/d = 1/2$, $t/d = 1/16$, $d = 25.4$ mm, $L = 300$ mm

1) Constants

$$\Gamma_1/ta^2d^3 = 2(1/24 + 1/8) - (1/4)(1/4)(1/4)2(2+2)(9/4)$$

$$\Gamma_1 = (5/96)ta^2d^3 = 218.535 \times 10^3 \text{ mm}^6$$

$$\mu = \sqrt{GJ/E\Gamma_1} = \sqrt{67.746/(3 \times 218.535 \times 10^3)} = 10.17 \times 10^{-3} \text{ mm}^{-1}$$

$$\mu L = 10.17 \times 10^{-3} \times 300 = 3.051$$

$$\exp(-2\mu L) = \exp(-6.102) = 2.25 \times 10^{-3}$$

2) Torsional Stiffness

$$\begin{aligned} T/\theta &= [\mu GJ(1 + \exp(-2\mu L))] / [(\mu L - 1) + (\mu L + 1)\exp(-2\mu L)] \\ &= [(10.17 \times 10^{-3}) \times (70 \times 10^3) \times 67.746(1 + 2.25 \times 10^{-3})] / [2.051 + (4.051 \times 2.25 \times 10^{-3})] \\ &= 23.457 \times 10^3 \text{ N} \cdot \text{mm/rad} = 23.48 \text{ N} \cdot \text{m/rad} \end{aligned}$$

3) Unconstrained Warping

$$\tilde{y}/d^2 = (1/2)(1/2)(1/2+1) / [2(1/2)+1] = 3/16$$

$$(GJ/T)w_1 = \tilde{y} = 3d^2/16$$

$$\therefore (GJ/Td^2)w_1 = 3/16$$

$$(GJ/T)w_3 = \tilde{y} - y_2 = 3d^2/16 - ad/2$$

$$\therefore (GJ/T)w_3 = 3/16 - (1/2)(1/2) = -1/16$$

Section B: $a/d = 4/7$, $t/d = 1/14$, $d = 44.45$ mm, $L = 1$ m

1) Constants

$$\Gamma_1/(ta^2d^3) = 2(4/84 + 1/8) - (1/4)(7/4)(15/4)(16/49)(121/49)/(225/49)$$

$$\Gamma_1 = 0.0571(ta^2d^3) = 10.28 \times 10^6 \text{ mm}^6$$

$$\mu = \sqrt{GJ/E\Gamma_1} = \sqrt{1016.19/(3 \times 10.28 \times 10^6)} = 5.7402 \times 10^{-3} \text{ mm}^{-1}$$

$$\mu L = 5.7402 \times 10^{-3} \times 1000 = 5.7402$$

$$\exp(-2\mu L) = \exp(-11.4804) = 10.33 \times 10^{-6}$$

2) Torsional Stiffness

$$\begin{aligned} T/\theta &= [\mu GJ(1 + \exp(-2\mu L))] / [(\mu L - 1) + (\mu L + 1)\exp(-2\mu L)] \\ &= [(5.7402 \times 10^{-3}) \times (70 \times 10^3) \times 1016.19(1 + 10.33 \times 10^{-6})] / [4.7402 + (6.7402 \times 10.33 \times 10^{-6})] \end{aligned}$$

$$T/\theta = 86.138 \times 10^3 \text{ N} \cdot \text{mm}/\text{rad} = 86.138 \text{ N} \cdot \text{m}/\text{rad}$$

3) Unconstrained Warping

$$\bar{y}/d^2 = (1/2)(4/7)(4/7+1)/[2(4/7)+1] = 22/105$$

$$(GJ/T)w_1 = \bar{y} = 22d^2/105$$

$$\therefore (GJ/Td^2)w_1 = 22/105$$

$$(GJ/T)w_3 = \bar{y} - y_2 = 22d^2/105 - ad/2$$

$$\therefore (GJ/Td^2)w_3 = 22/105 - (1/2)(4/7) = -0.0762$$

Section C: $a/d = 1/3$, $t/d = 1/40$, $d = 47.625 \text{ mm}$, $L = 340 \text{ mm}$

1) Constants

$$\Gamma_1/(ta^2d^3) = 2(1/36 + 1/8) - (1/4) \times 3(2+3)(1/9)(4/3)^2/(25/9)$$

$$\Gamma_1 = 0.0389ta^2d^3 = 1.2605 \times 10^6 \text{ mm}^6$$

$$\mu = \sqrt{GJ/E\Gamma_1} = \sqrt{44.657/(3 \times 1.2605 \times 10^6)} = 3.436 \times 10^{-3} \text{ mm}^{-1}$$

$$\mu L = 3.436 \times 10^{-3} \times 340 = 1.168$$

$$\exp(-2\mu L) = \exp(-2.336) = 0.0967$$

2) Torsional Stiffness

$$\begin{aligned} T/\theta &= [\mu GJ(1 + \exp(-2\mu L))]/[(\mu L - 1) + (\mu L + 1)\exp(-2\mu L)] \\ &= [(3.436 \times 10^{-3}) \times (70 \times 10^3) \times 44.657(1 + 0.0967)]/[0.168 + (2.168 \times 0.0967)] \\ &= 31.203 \times 10^3 \text{ N} \cdot \text{mm}/\text{rad} = 31.2 \text{ N} \cdot \text{m}/\text{rad} \end{aligned}$$

3) Unconstrained Warping

$$\bar{y}/d^2 = [(1/2)(1/3)(4/3)/(2/3+1)]/[2(4/7)+1] = 2/15$$

$$(GJ/T)w_1 = \bar{y} = 2d^2/15$$

$$\therefore (GJ/Td^2)w_1 = 2/15$$

$$(GJ/T)w_3 = \bar{y} - y_2 = 2d^2/15 - ad/2 = 2/15 - (1/2)(1/3)$$

$$\therefore (GJ/Td^2)w_3 = -1/30$$

With the torque applied at O, the free (unconstrained) warping displacement is constant in the web. Comparisons between free warping displacements from torsion applied about axis E and from torsion applied about axes G and O are as shown for all sections in **Figures 5(a)-(c)**.

The ordinates for points 1, 3 and 4 in each section with the torque applied at E, G and O are given in non-dimensional form in **Table 6**. Here the non-dimensional displacements appear in multiples of the square dimension a^2 , these allowing the physical displacements to be calculated for points 1, 3 and 4 in channel sections A, B and C as required. For example, at the neutral axis (point 4) the warping displacement under a torque of 1 Nm applied to section B ($a/d = 4/7$) are found from **Table 6** as follows:

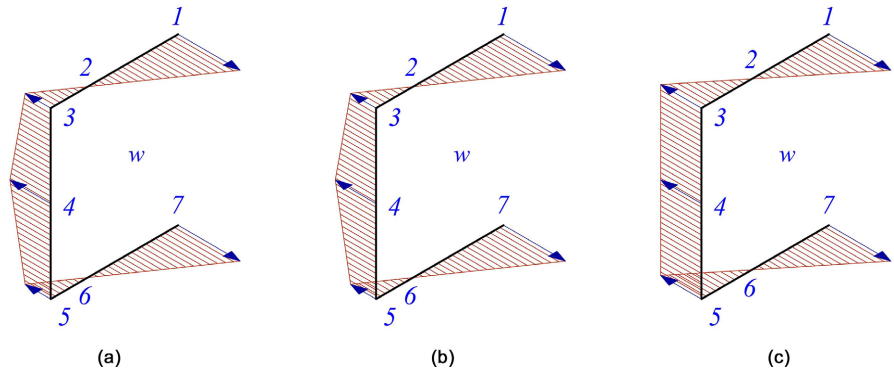


Figure 5. Influence of the longitudinal axis of torsion upon the unconstrained warping displacements for all channel sections: Axes: (a) shear centre E, (b) centroid G and (c) web centre O.

at E: $GJw/T = -0.493a^2$

$$w = -0.493a^2T/JG = -0.493 \times 25.4^2 \times (1 \times 10^3) / (1016.2 \times 70 \times 10^3) = -4.475 \times 10^{-3} \text{ mm}$$

at G: $GJw/T = -0.414a^2$

$$w = -0.414a^2T/JG = -0.414 \times 25.4^2 \times (1 \times 10^3) / (1016.2 \times 70 \times 10^3) = -3.758 \times 10^{-3} \text{ mm}$$

at O: $GJw/T = -0.233a^2$

$$w = -0.233a^2T/JG = -0.233 \times 25.4^2 \times (1 \times 10^3) / (1016.2 \times 70 \times 10^3) = -2.115 \times 10^{-3} \text{ mm}$$

3.3. Fixed-End Stress Distributions

The shift in the axis of torsion from E to O influences the fixed end axial stress distribution. For torque T , concentric with the web centre axis O, the stress constraint is found from Equation (8) with a change appropriately to \tilde{y} and T_i . For example, these give for channel section A:

$$\begin{aligned} \sigma_z &= [(\tilde{y} - y)T/\mu\Gamma_1] \times (1 - \exp(-2\mu L)) / (1 + \exp(-2\mu L)) \\ &= [(\tilde{y} - y)T / (0.8887t/a^2) \times (0.4166a^5t)] \times (1 - \exp(-5.248)) / (1 + \exp(-5.248)) \end{aligned}$$

which is re-arranged as:

$$(a^3t^2/T)\sigma_z = 2.6726(3a^2/4 - y)$$

where y is taken from the swept area diagram (see **Figure 4(b)**) for perimeter points 1, 3 and 4:

$$y_1 = 0, (a^3t^2/T)\sigma_{z1} = 2.6726(3a^2/4)$$

$$\therefore at^2/\sigma_{z1} = 2.004$$

$$y_3 = ad/2, (a^3t^2/T)\sigma_{z3} = 2.6726(3a^2/4 - ad/2)$$

$$\therefore at^2/\sigma_{z3} = -0.6682$$

$$y_4 = ad/2, \quad (a^3t^2/T)\sigma_{z3} = 5.345(3a^2/4 - ad/2)$$

$$\therefore (at^2/T)\sigma_{z3} = -0.6682$$

which shows that the compression in the web is uniform, this repeating the flat swept area feature in the diagram of **Figure 4(b)**. Because similar constrained stress distributions will apply to the channel sections B and C it is sufficient to reveal their common trend in **Figure 6** for section A only below

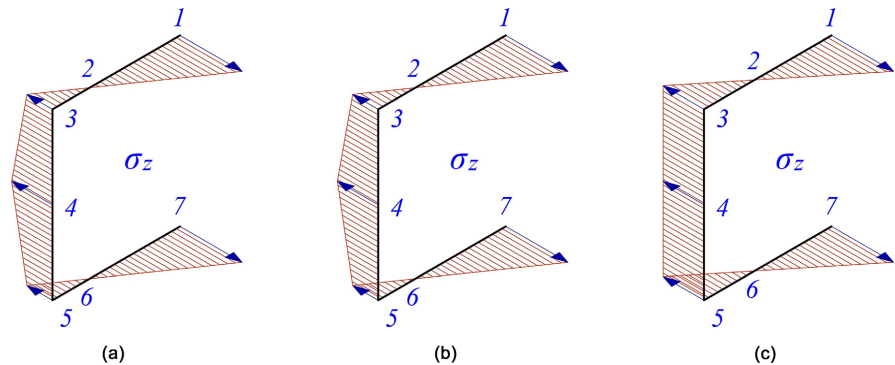


Figure 6. Influence of the longitudinal axis of torsion upon the fixed-end stress state for channel section A. Axes: (a) shear centre E, (b) centroid G and (c) web centre O.

The non-dimensional plots (a)-(c) in **Figure 6** appear in three oblique views which show points of maximum tension and compression at the flange ends (point 1 and 7) and web centre (point 4) respectively. Distribution (c) differs in showing uniform compression in the web. The stress magnitudes may be checked for the non-dimensional co-ordinate calculated for a unit torque (1 Nm) below. Thus, the greatest tension and compression at points 1 and 4 across the three diagrams are converted to stress magnitudes as follows:

$$\begin{aligned} \text{a) } (at^2/T)\sigma_{z1} &= 1.53, \quad \therefore \sigma_{z1} = (1.53 \times 1000) / (12.7 \times 1.5875^2) = 47.8 \text{ MPa} \\ (at^2/T)\sigma_{z4} &= -0.9634, \\ \therefore \sigma_{z4} &= (-0.9634 \times 1000) / (12.7 \times 1.5875^2) = -30.1 \text{ MPa} \\ \text{b) } (at^2/T)\sigma_{z1} &= 1.5937, \\ \therefore \sigma_{z1} &= (1.5937 \times 1000) / (12.7 \times 1.5875^2) = 49.79 \text{ MPa} \\ (at^2/T)\sigma_{z4} &= -0.8582, \\ \therefore \sigma_{z4} &= (-0.8582 \times 1000) / (12.7 \times 1.5875^2) = -26.81 \text{ MPa} \\ \text{c) } (at^2/T)\sigma_{z1} &= 2.004, \quad \therefore \sigma_{z1} = (2.004 \times 1000) / (12.7 \times 1.5875^2) = 62.61 \text{ MPa} \\ (at^2/T)\sigma_{z4} &= -0.6682, \\ \therefore \sigma_{z4} &= (-0.6682 \times 1000) / (12.7 \times 1.5875^2) = -20.88 \text{ MPa} \end{aligned}$$

which all appear as elastic stresses for the stated unit torque value.

4. Summary of Constrained Behaviour

Here the trends made apparent from the specific calculations given above are

assembled. To understand the full effect of the fixed-end constraint, first, the unconstrained torsional warping displacements are required. When that warping is constrained, in this case by one end fixing, there are three influences that have appeared under an axial torsion. The fixing serves to: (i) modify the free warping displacement distribution, (ii) induce axial stress and (iii) alter the torsional stiffness. Moreover, it has been shown that (i), (ii) and (iii) are sensitive to the axis of that torque as demonstrated above for axes through the shear centre **E**, the centroid **G** and web-centre **O**.

4.1. Unconstrained Warping

Figures 5(a)-(c) showed the warping displacement distribution at the free end of each channel section. Consistently, for $w_3 = w_4 = w_5$, the full web depth displaces inwardly by a constant compression for an axis at **O**. This displacement is matched by a linear warping distribution with each flange at corners 3 and 5 where an outward displacement applies to the section's free ends 1 and 7. With the symmetry that appears in warping displacements it is sufficient to refer distributions in each section to points 1, 3 and 4 for when the torque is shifted from a longitudinal axis passing through the shear centre **E** to one through the web centre **O** and then to another axis through the centroid **G**. **Table 6** summarises the normalised unconstrained displacements given as: GJw/Ta^2 , for sections **A**, **B** and **C** from the calculations given above.

Table 6. Dependence of unconstrained normalised warping displacements GJw/Ta^2 upon the torsion axis.

↓ Point	Section A, Axes ↓			Section B, Axes ↓			Section C, Axes ↓		
	E	O	G	E	O	G	E	O	G
1	27/32	3/4	13/16	0.721	0.642	0.696	27/20	1.2	1.29
3	-5/32	-1/4	-3/16	-0.154	-0.233	-0.179	-3/20	-0.3	-0.21
4	-17/32	-1/4	-7/16	-0.493	0.233	-0.414	-13/20	-0.3	-0.51

Table 6 shows that warping displacements in each section do not increase with axis shift from the shear centre. In fact, the displacements are the greatest for points 1 and 4 and the least for point 3 with torque applied at the shear centre. Minimum displacement applies to corner points 3 in all sections.

Note: Unconstrained warping displacements, calculated from swept areas, are independent of the beam length.

4.2. Constrained Axial Stress

The constrained axial stress is induced when one end is prevented from warping but with the other end free to warp partially. There is a similarity in the free warping displacement distribution when a torque is applied about axes **E**, **G** and **O** for the three different channel sections given above. Therefore, it is sufficient to refer the constrained axial stress distribution to the axis **E** [1] given in **Table 7**.

It follows that axial stress will be distributed similarly to Fig. 6 but with a change to its magnitude following a shift in the axes of torsion from **E** to **G** and from **E** to **O**.

Table 7. Conversion of normalised axial stress $(at^2/T)\sigma_z$ at median points 1, 3 and 4 to (MPa) for three channel cross-sections **A**, **B** and **C** with torque applied at **E**.

Section ($a \times t$) → Position ↓	A: 1/2" × 1/16"	B: 1" × 1/8"	C: 5/8" × 3/64"
1	1.530 (47.80)	1.5978 (6.24)	1.004 (44.61)
3	-0.2834 (-8.85)	-0.3421 (-1.34)	-0.1171 (-5.20)
4	-0.9634 (-30.10)	-1.093 (-4.27)	-0.5076 (-22.55)

The entries given in **Table 7** along with the section dimensions ($a \times t$) allow a calculation of the stress magnitude (given as MPa in brackets). For example, if a 'unit' torque of 1 Nm is applied across the top line, then the normalised stress entries of 1.530, 1.5978 and 1.004 at position 1 for channel sections **A**, **B** and **C** are converted to MPa as follows:

$$\sigma_z = 1.53T/at^2 = (1.53 \times 1000) / \left((1/2) \times (1/16^2) \times 25.4^3 \right) = 47.8 \text{ MPa}$$

$$\sigma_z = 1.5978T/at^2 = (1.5978 \times 1000) / \left(1 \times 1/8^2 \times 25.4^3 \right) = 6.24 \text{ MPa}$$

$$\sigma_z = 1.004T/at^2 = (1.004 \times 1000) / \left(5/8 \times (3/64)^2 \times 25.4^3 \right) = 44.61 \text{ MPa}$$

Under this unit torque such stress magnitudes may be borne by an aluminium alloy channel at the fixing without yielding occurring, given that they diminish to zero at the free end.

4.3. Torsional Stiffness

Table 8 compiles the torsional stiffness for the three sections with the axis of torsion passing through points **E**, **G** and **O**. It is seen that an axis shift alters the Wagner-Kappus stiffness [11] [12] but not the St Venant stiffness [9] [10]. Pure torsion (St Venant's) applies to each axis in the case of unconstrained ends. That is, pure torsion arises from an end couple placed anywhere along the horizontal x -axis of symmetry. In the case of constraining one end fully to prevent twist then a free-end torque provides a maximum torsional stiffness (Wagner-Kappus) only when applied through the axis **E**.

Table 8 shows that torsion applied about any other axis (e.g. **G** and **O**) involves a contribution from bending with reduced stiffness. The interplay between section geometry and beam length appears in the central column in which every stiffness with an end fixing can be seen to exceed the St Venant's stiffness for a beam with both ends free.

4.4. Constrained Warping

The influence of fixing one end upon the warping displacements at the ends and

Table 8. Comparison between Wagner-Kappus and St Venant Torsional Stiffness (Nm/rad).

Section	Axes	$(T\theta)_{W-K}$	$(T\theta)_{StV}$
A: 1/2" × 1" × 1/16" × 300 mm	E	26.67	
	G	25.44	15.81
	O	23.48	
B: 1" × 1 3/4" × 1/8" × 1 m	E	91.18	
	G	89.42	71.18
	O	86.14	
C: 5/8" × 1 7/8" × 3/64" × 340 mm	E	39.79	
	G	37.32	9.19
	O	31.20	

centre of the beam has been considered with the torque applied through points **E**, **G** and **O** of each channel section. For each application it is clear that the displacement is eliminated at the fixing and reduced elsewhere in the length. The end constraint extends to the free end where warping under torsion is less than that found with both ends free. **Table 9** establishes the hyperbolic distribution of constrained warping for channel section a with torque applied about axis **E**. Equation (7) is applied as follows

$$w/w_o = 1 - [\cosh 2.618(1 - z/L)]/6.857$$

giving w/w_o for eleven length positions z/L as in **Table 9**.

Table 9. Constrained warping for channel section **A** at one tenth length positions.

z/L	0	0.1	0.2	0.3	0.4	0.5	0.6	0.7	0.8	0.9	1.0
w/w_o	0	0.227	0.401	0.534	0.635	0.711	0.767	0.807	0.833	0.849	0.854

The coefficients w/w_o are section-dependent. Those given for section a in **Table 9** are to be multiplied by the free warping displacements w_o for points 1, 3 and 4 etc. at the corresponding length position. The conversion to physical displacement w for the three sections at these positions for end and centre has been outlined earlier from **Tables 1-3**.

4.5. Trans-Moment

Some analyses express the constrained axial stress in terms of a *bimoment* [4] but here this stress has been calculated directly from any one of Equations 9(a)-(c). The net stress given in Figs should agree by either approach but there is one further contribution to this net stress that might be influential. That is where a moment transfer is introduced in providing a possible further contribution to the net axial stress. The trans-moment has its counterpart within the static equivalence that applies when a vertical transverse force F_y is shifted from its posi-

tion within the cross section, say from **G**, to the shear centre **E** [1]. That force transfer must be accompanied by a torque that is the product $T = F_y(e_x + X')$, where in a channel section, $(e_x + X')$, is the horizontal perpendicular distance between parallel vertical axes through **G** and **E**. Here distances X' and e_x lie on either side of the web centre respectively. So too, when a bending moment M_y is shifted from acting about its vertical axis y through **G** to a vertical axis through **E**, that moment must be accompanied by a corresponding trans-moment $M = M_y(e_x + X')$ [2] [3] [4]. This trans-moment is examined in more detail [13] where it is suggested how it is converted into a uniform axial stress that is to be superimposed upon the axial stress distributions arising from flexural bending and from the constrained warping.

5. Conclusions

The position of the shear centre **E** in an x -symmetric channel section lies upon the x -axis and is separated from the centroid **G** by a known distance upon the same axis. Both **E** and **G** are properties of the channel as defined by its geometry. With an axis of torsion taken at **G** and then at the web centre **O**, the results show that respective unconstrained warping displacements differ from applying torsion about the axis at **E** in channel section cantilever beams with free ends. Moreover, with one beam end fixed to eliminate axial warping, the constrained axial stress distribution diagrams at the fixing differ between the three axes. These constrained stress mirrors in proportion the unconstrained warping displacement that would arise when the constraint is released. Differences between these distributions are attributed to rotating axes of torsion passing through **G** and **O** over the length. It is believed that the displacements at a point in the cross section, as they arise from its rotation in the section and warping in the length, are attributed to bending under a moment that varies with the beam length. With that moment variation, it is suggested that transverse shear arises as the moment's derivative with respect to length.

Thus, torsion applied to any arbitrary longitudinal axis is likely to introduce a bending contribution that would otherwise be absent for torsion applied to the flexural axes.

Conflicts of Interest

The authors David Rees, and Abdelraouf Alsheikh, have received research support from the Department of Design. The authors declare that they have no conflict of interest.

References

- [1] Rees, D.W.A. and Alsheikh, A.M.S. (2024) Theory of Flexural Shear, Bending and Torsion for a Thin-Walled Beam of Open Section. *World Journal of Mechanics*, **14**, 23-53. <https://doi.org/10.4236/wjm.2024.143003>
- [2] Vlasov, V.Z. (1961) *Thin-Walled Elastic Beams*. Oldbourne Press.
- [3] Al-Sheikh, A.M.S. (1985) *Behaviour of Thin-Walled Structures under Combined*

- Loads. Ph.D. Thesis, Loughborough University of Technology.
- [4] Alsheikh, A.M.S. and Rees, D.W.A. (2021) General Stiffness Matrix for a Thin-Walled, Open-Section Beam Structure. *World Journal of Mechanics*, **11**, 205-236. <https://doi.org/10.4236/wjm.2021.1111015>
- [5] Hoff, N.J. (1943) Stresses in Space-Curved Rings Reinforcing the Edges of Cut-Outs in Monocoque Fuselages. *The Journal of the Royal Aeronautical Society*, **47**, 35-83. <https://doi.org/10.1017/s0001924000100818>
- [6] Gjelsvik, A. (1981) *The Theory of Thin-Walled Beams*. Wiley.
- [7] Williams, D. (1960) *Theory of Aircraft Structures*. E. Arnold.
- [8] Bleich, F and Bleich, H.H. (1952) *Buckling Strength of Metal Structures*. McGraw-Hill.
- [9] Rees, D.W.A. (2016) *Mechanics of Solids and Structures*. 2nd Edition, IC Press.
- [10] Megson, T.H.G. (1972) *Aircraft Structures for Engineering Students*. E. Arnold.
- [11] Wagner, H. (1936) NACA, US. T.M. No. 807.
- [12] Boresi, A.P., Schmidt, R.J. and Sidebottom, O.M. (1993) *Advanced Mechanics of Materials*. John Wiley and Sons.
- [13] Rees, D.W.A. and Al-Sheikh, A.M.S. (2024) The Longitudinal Axis of Loading Thin-Walled Beams of Open Section: Combined Flexural Shear, Bending and Torsion of a Cantilever Channel. *Engineering*, in press.

List of Symbols

a, d, t	cross-section dimensions
A	cross-sectional area
X'	centroid position
I_1	primary warping constant
J	St Venant torsion constant
μ	warping constant
θ	angular twist
T	axial torque
G	shear modulus, $G = 70$ GPa
E	modules of elasticity, $E = 210$ GPa
w	constrained warping displacement
w_o	unconstrained warping displacement
σ_z	axial stress
y	swept area ordinate
\bar{y}	swept area centroid
z	length co-ordinate